RSC Advances

PAPER

View Article Online
View Journal | View Issue

Cite this: *RSC Adv.*, 2021, **11**, 13341

A ratiometric fluorescent probe for the detection of β-galactosidase and its application†

Yanan Li, Bing Deng, Haitao Chen, * Shaoxiang Yang * and Baoguo Sun

Received 28th January 2021
Accepted 1st April 2021

DOI: 10.1039/d1ra00739d

rsc.li/rsc-advances

Herein, a coumarin fluorescent probe (Probe **1**) was developed for the ratiometric detection of β-galactosidase (β-gal) activity. The detection range was 0–0.1 U mL^{-1} and 0.2–0.8 U mL^{-1}, and the limit of detection (LOD) was 0.0054 U mL^{-1}. Moreover, the luminous intensity of Probe **1** increased gradually with increase in β-gal activity. It could be observed under 254 nm UV irradiation by the naked eye. Furthermore, this method only required a small amount of sample (20 μL) and a short analytical time (30 min) for the detection of β-gal activity with a low LOD. Probe **1** was successfully used to detect β-gal activity in real fruit samples, and can be applied to the quantitative and qualitative detection of β-gal activity.

1. Introduction

β-Galactosidase (β-gal, EC 3.2.1.23) is part of the glycoside hydrolase family and has many microbial sources.[1] In addition to its hydrolysis activity, β-gal from some sources also exhibits glycosylation activity. Food-processing applications of β-gal mainly include the following: allowing lactose-intolerant individuals to consume dairy; improving the sweetness of dairy products; preventing dairy products from crystallizing during freezing; the production of galactooligosaccharides; applications in fermented dairy products; whey processing; the analysis of lactose content in dairy products; and promoting the softening and ripening of fruit and vegetables.[2–4] β-gal has also been used for improving the sweetness, digestibility, flavor, and solubility of dairy products.[5]

β-Galactosidase is widely found in many kinds of plants. Generally, the content of β-gal increases when plants mature,[6] and the activity of β-gal has a positive correlation with the maturity of fruit, including tomato,[7] papaya,[8] apple,[9] persimmon,[10] kiwi fruit,[11] avocado,[12] pear,[13] peach,[14] and mango.[15] It can degrade cell-wall polysaccharides and release free galactose, which can promote – for example – pepper ripening and ethylene production in tomatoes.[7] However, many enzymes exist in different types of fruit. Therefore, the development of a simple, selective, and rapid detection method for β-gal activity in fruit is important.

To date, many methods have been used for the detection of β-gal activity. These include chemiluminescence,[16] HPLC,[17] colorimetric methods,[18] magnetic resonance,[19] UV spectrophotometry,[20] positron emission tomography,[21] enzyme-linked immunosorbent assay technology,[22] and electrochemical methods.[23] However, there are certain disadvantages associated with these methods, such as long experimental duration, complex operation conditions, and high experimental costs. Thus, developing a selective, rapid, and simple detection method for β-gal activity is necessary for applications in fruit production. To this end, the development of novel fluorescent probes is very promising,[24–29] and many kinds of β-gal probes have been reported for use in biological imaging,[30–32] including two-photon fluorescence probes,[33,34] ratiometric probes,[35,36] and turn-on probes.[37–39] However, fluorescent probes used in fruit detection are extremely rare in scientific literature.[40,41]

To develop a simple detection method for β-gal activity in fruit, a ratiometric fluorescent probe (Probe **1**) with high accuracy and detection precision was developed. This ratiometric fluorescent probe has the characteristics of high accuracy and strong anti-interference. Further, the luminous intensity of the Probe **1** solution increased with increasing β-gal activity under 254 nm UV irradiation. In addition, Probe **1** was successfully applied to the quantitative and qualitative detection of β-gal activity in fruit.

2. Materials and methods

2.1 General methods

The β-gal, sodium chloride (NaCl), magnesium chloride ($MgCl_2$), hydrogen peroxide (H_2O_2), ammonium chloride (NH_4Cl), sodium bromide (NaBr), glutathione (GSH, 98%), glycine (Gly), D-leucine (Leu), potassium iodide (KI), histidine (His), potassium chloride (KCl), L-valine (Val), β-glucuronidase (from *Escherichia coli*), lysozyme (from chicken egg whites), lipase (from porcine pancreas), and α-galactosidase (α-gal) were purchased from Bailingwei Co., Ltd, China.

Beijing Key Laboratory of Flavor Chemistry, Beijing Technology and Business University, Beijing 100048, China. E-mail: chenht@th.btbu.edu.cn; yangshaoxiang@th.btbu.edu.cn

† Electronic supplementary information (ESI) available. See DOI: 10.1039/d1ra00739d

2.2 Instruments

Fluorescence spectra were obtained using the Rili F-4600 fluorescence spectrometer. NMR spectra were obtained using the Bruker AV 300 MHz NMR machine. HRMS was performed using a Bruker Apex IV FTMS.

2.3 Synthesis of Probe 1

7-Hydroxy-4-methylcoumarin (0.18 g, 1.00 mmol), Cs_2CO_3 (1.63 g, 5.00 mmol), Na_2SO_4 (0.36 g, 2.50 mmol), galacto-pyranosyl-1-bromide (3068-32-4, 0.31 g, 0.75 mmol), and CH_3CN (30 mL) were added to a flask (Scheme 1) and reacted for 1 h at 25 °C to obtain compound **2** (0.35 g, 91% yield).

Compound **2** (0.23 g, 0.4 mmol) was dissolved in CH_3OH (20 mL). A solution of K_2CO_3 (0.13 g, 0.09 mmol) and CH_3OH (80 mL) was added and reacted for 4 h at 25 °C, after which the mixture was adjusted to pH 7 using an aqueous H_2SO_4 solution (0.05 M). The precipitate was removed by filtration and recrystallized from ethanol to obtain Probe **1** (0.11 g, 81% yield).

^{1}H NMR (300 MHz, $CDCl_3$) δ (ppm): 7.70 (d, J = 9.4 Hz, 1H), 7.03 (d, J = 7.0 Hz, 2H), 6.24 (s, 1H), 5.21 (s, 1H), 4.98 (d, J = 7.6 Hz, 1H), 4.87 (s, 1H), 4.66 (s, 1H), 4.52 (s, 1H), 3.72 (s, 1H), 3.66 (d, J = 6.1 Hz, 1H), 3.60 (d, J = 8.1 Hz, 1H), 3.53 (s, 2H), 3.45 (s, 1H), 2.41 (s, 3H). ^{13}C NMR (75 MHz, $CDCl_3$) δ (ppm): 160.23, 160.06, 154.39, 153.28, 126.35, 113.99, 113.40, 111.62, 103.17, 100.64, 75.69, 73.20, 70.09, 68.11, 60.37, 18.08. HRMS (ESI): calcd for $[M - H]^-$ 337.092891, found 337.0931.

2.4 Preparation of analytes

Probe **1** was dissolved using DMSO. β-gal, β-glucuronidase, lysozyme, lipase, and α-gal were dissolved in Tris–HCl (pH 7.3, 50 mM) and frozen in a −20 °C refrigerator. The stock solution was diluted using a certain concentration gradient with Tris–HCl (pH 7.3, 50 mM) before each use. NaCl, KCl, $MgCl_2$, KI, NH_4Cl, NaBr, H_2O_2, GSH, Gly, Leu, His, and Val, were dissolved in deionized water.

2.5 Preparation of samples

Pears, apples, grapes, strawberries, and kiwis were bought from a local supermarket. Twenty grams of the abovementioned fruit were centrifuged for 10 min, at 12 000 rpm, after grinding; subsequently, the supernatant was obtained, which was filtered and reserved.

2.6 Fluorescence detection assays

The Probe **1** solution (1 mM, 0.02 mL) was added to a cuvette, to which 2 mL of water was added. Then, β-gal was added; after 40 min, the mixture was analyzed using fluorescence spectra (slit width = 5 nm, λ_{ex} = 327 nm, voltage = 500 V, and temperature = 37 °C).

3. Results and discussion

3.1 Probe preparation

Probe **1** was synthesized in two steps. First, compound **2** was obtained through the nucleophilic substitution of 7-hydroxy-4-methylcoumarin with galacto-pyranosyl-1-bromide (3068-32-4). Second, the acetyl groups of compound **2** were hydrolyzed to obtain Probe **1** (Scheme 1). Probe **1** was purified by recrystallization from ethanol, and NMR and HRMS were used to characterize this probe (Fig. S1–S3, ESI†). The preparation process was carried out at 25 °C under mild conditions; thus, the synthesis of Probe **1** was a simple process.

3.2 Fluorescence properties

First, the fluorescence response of Probe **1** with β-gal in different solutions (CH_3CN, H_2O, DMSO, C_2H_5OH, and THF) was determined (Fig. 1a). After the addition of β-gal, the fluorescence intensity was decreased at 374 nm in CH_3CN, DMSO, C_2H_5OH, and THF, with changes in only one fluorescent emission. In H_2O, however, the fluorescence intensity was decreased at 374 nm and significantly increased at 444 nm. As shown in Fig. 1b, Probe **1** displayed a fluorescence emission peak at 374 nm in an H_2O solution. After the addition of β-gal, the fluorescence intensity at 374 nm decreased and a peak appeared at 444 nm. The fluorophore (7-hydroxy-4-methylcoumarin, compound **1**) had a peak at 444 nm in an H_2O solution. This confirmed that 374 nm was the peak of Probe **1** and 444 nm was the fluorescence-emission peak of the fluorophore. These results indicated that Probe **1** was

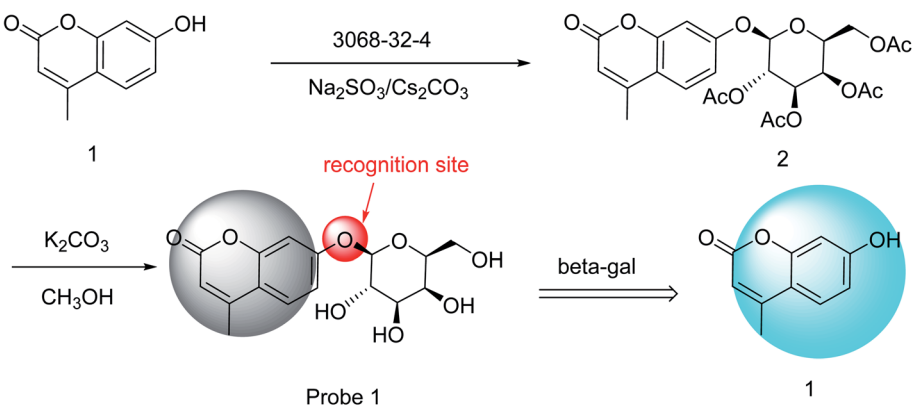

Scheme 1 Synthesis of Probe **1** and the recognition mechanism of Probe **1** to β-gal.

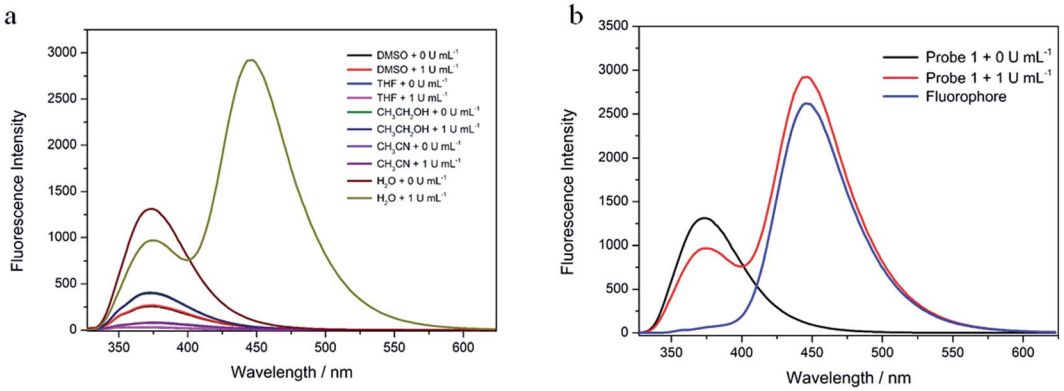

Fig. 1 (a) Fluorescence spectra of Probe **1** (10 μM) and Probe **1** in the presence of β-gal (1 U mL^{-1}) in CH_3CN, H_2O, DMSO, C_2H_5OH and THF at 37 °C. (b) Fluorescence spectra of Probe **1** (10 μM), compound **1** (10 μM) and Probe **1** in the presence of β-gal (1 U mL^{-1}) in H_2O at 37 °C.

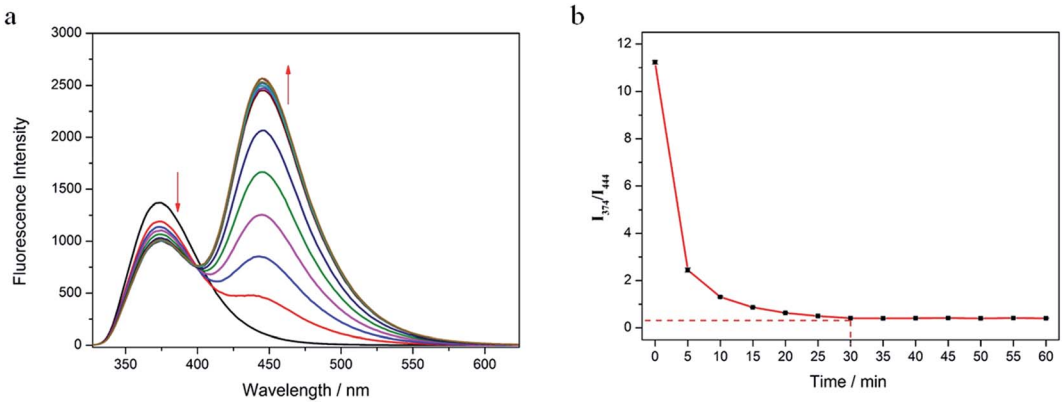

Fig. 2 (a) Time-dependent fluorescence spectra of Probe **1** (10 μM) in the presence of β-gal (1 U mL^{-1}) in water at 37 °C. (b) The fluorescence emission ratio ($I_{444\ nm}/I_{374\ nm}$) of Probe **1** in the presence of β-gal form 0 min to 60 min. Tests were performed in triplicate.

a ratiometric probe, facilitating the detection of β-gal by determining the ratio of fluorescence intensity at two different emission wavelengths.

Second, the time-response relationships of Probe **1** toward β-gal in water were tested (Fig. 2a). The fluorescence intensity at 374 nm decreased slowly with the addition of β-gal. Simultaneously, the fluorescence intensity at 444 nm increased rapidly. The fluorescence emission ratio ($I_{444\ nm}/I_{374\ nm}$) decreased rapidly from 0 to 10 min, and reached an equilibrium in 30 min (Fig. 2b). The emission ratio remained unchanged from 30 to 60 min. This shows that 30 min were required for the identification of β-gal by Probe **1**, which was set as the duration for the subsequent experiments.

The effects of competitor ions and compounds were used to ascertain the selectivity of Probe **1**. Various competitors were tested, including Na^+, K^+, Mg^{2+}, I^-, NH_4^+, Br^-, H_2O_2, Cl^-, GSH, Gly, Leu, Val, His, β-glucuronidase, lipase, and lysozyme (Fig. 3). In the presence of any of these competing ions and compounds, there was minimal change in the emission ratio ($I_{444\ nm}/I_{374\ nm}$). In particular, Probe **1** was almost unresponsive in the presence of β-glucuronidase and α-gal. However, with the addition of β-gal, the emission ratios ($I_{444\ nm}/I_{374\ nm}$) of Probe **1** + β-gal and Probe **1** + β-gal + competitors were

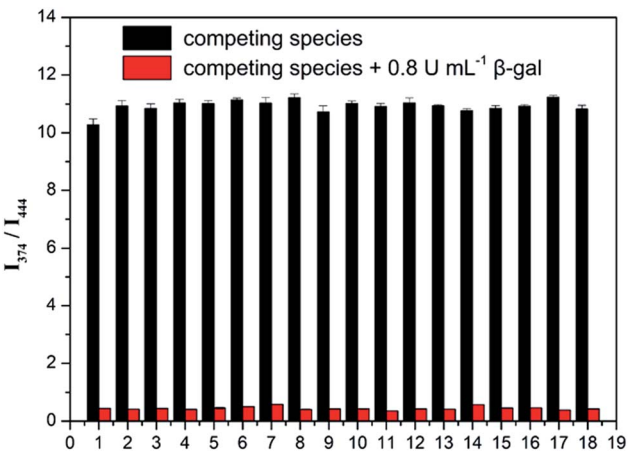

Fig. 3 The fluorescence emission ratio ($I_{444\ nm}/I_{374\ nm}$) of Probe **1** (10 μM) upon addition of various species (0.8 U mL^{-1} for α-gal, lipase and 100 μM for others. 1, blank; 2, Na^+; 3, K^+; 4, Mg^{2+}; 5, I^-; 6, NH_4^+; 7, Br^-; 8, H_2O_2; 9, GSH; 10, Gly; 11, Leu; 12, His; 13, Val; 14, β-glucuronidase; 15, lysozyme; 16, lipase; 17, α-gal; 18, Cl^-. 0.8 U mL^{-1} for β-gal). Tests were performed in triplicate.

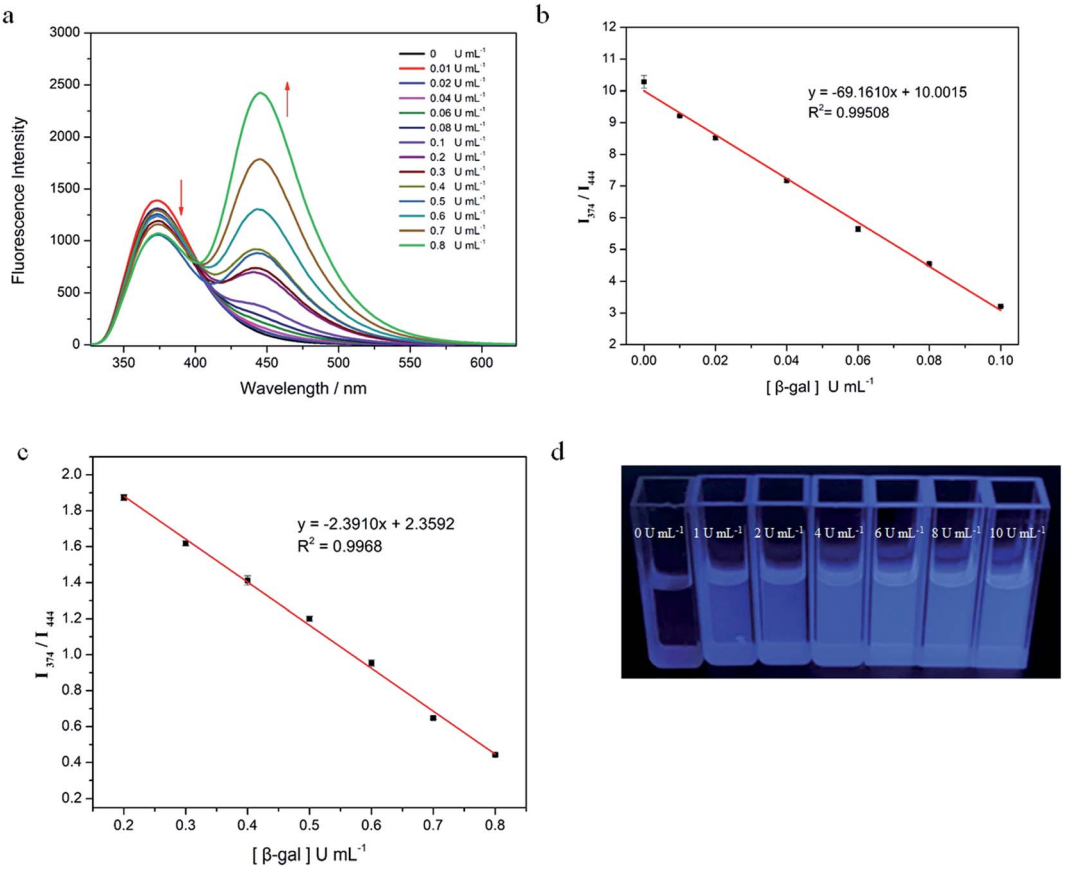

Fig. 4 (a) Fluorescence spectra of Probe **1** (10 μM) with β-gal (0, 0.01, 0.02, 0.04, 0.06, 0.08, 0.1, 0.2, 0.3, 0.4, 0.5, 0.6, 0.7, 0.8 U mL^{-1}). (b) Plot of fluorescence intensity differences with 0–0.1 U mL^{-1} β-gal. (c) Plot of fluorescence intensity differences with 0.2–0.8 U mL^{-1} β-gal. Tests were performed in triplicate. (d) Photograph of Probe **1** (10 μM) luminescent intensity subjected to β-gal (0, 1, 2, 4, 6, 8, 10 U mL^{-1}) under 254 nm UV light.

almost identical. This indicates that Probe **1** has high selectivity in detecting β-gal.

The fluorescence-intensity changes of Probe **1** with various activities of β-gal (0, 0.01, 0.02, 0.04, 0.06, 0.08, 0.1, 0.2, 0.3, 0.4, 0.5, 0.6, 0.7, and 0.8 U mL^{-1}) were recorded and are shown in Fig. 4a. The emission ratio ($I_{444\ nm}/I_{374\ nm}$) exhibited two linear sections in response to β-gal activity: 0–0.1 U mL^{-1} (R^2 = 0.9951, Fig. 4b) and 0.2–0.8 U mL^{-1} (R^2 = 0.9968, Fig. 4c). The Probe **1** limit of detection (LOD) for β-gal activity was 0.0054 U mL^{-1}, based on LOD = 3 SD/B. This indicated that Probe **1** could be used to detect β-gal activity with a low LOD in water. In addition, the luminous intensity of Probe **1** gradually increased with increases in β-gal activity, as was observed by the naked eye under 254 nm UV irradiation (Fig. 4d). All results showed that Probe **1** could be used as a quantitative and qualitative tool to detect β-gal activity.

3.3 Recognition mechanism

After the addition of β-gal (1 U mL^{-1}), a new peak appeared, which was previously proven to be compound **1** (Fig. S4, ESI†). Mass spectrometry provided further evidence that the β-galactosides were hydrolyzed (Fig. S5, ESI†), with the peak at m/z = 174.56.00 corresponding to compound **1** (M − H); the peak at m/z = 337.04 was that of Probe **1** (M − H). These results show that Probe **1**'s mechanism for β-gal recognition is the β-gal enzymatic hydrolysis of β-galactosides.

3.4 Application

As β-gal activity is positively correlated with the maturity of fruit, the development of a simple and highly selective method for β-gal activity detection in fruit is crucial. Therefore, the ability of Probe **1** to detect β-gal activity in fruit must be demonstrated.

Pear, apple, grape, strawberry, and kiwi (20 μL) samples were tested using Probe **1**. The β-gal activity of the kiwi (ripe) sample was 0.0938 ± 0.0027 U mL^{-1}, and those of the kiwi (unripe), pear, apple, grape, and strawberry samples were 0 U mL^{-1} (Table 1). The ripeness of the kiwi fruit was mainly determined by the softness or hardness of the fruit (Fig. S6, ESI†).

To validate this method, the β-gal activity in these samples was tested using the β-galactosidase spectrophotometric method.[40,41] The β-gal activity of all samples was 0 U mL^{-1}. No β-gal activity was detected in the kiwi (ripe) sample by the GB/T 33409-2016 method; this could be because the β-gal activity in kiwis (ripe) and the LOD of this method are of the same order of magnitude. Then, the addition of β-gal with different activities (0.02, 0.04, 0.2, and 0.4 U mL^{-1}) to the samples showed that the

Table 1 Determination of β-gal activity in real fruit samples

Sample	β-gal level found (U mL^{-1})	Added (U mL^{-1})	Found (U mL^{-1})	Recovery/%	RSD/% ($n = 3$)
Pear	0	0.02	0.022	108.00	0.11
		0.04	0.043	106.61	0.21
		0.2	0.221	101.32	1.69
		0.4	0.405	101.33	1.44
Apple	0	0.02	0.022	110.29	0.07
		0.04	0.044	108.94	0.33
		0.2	0.192	96.13	2.09
		0.4	0.387	96.71	6.31
Grape	0	0.02	0.022	108.80	0.26
		0.04	0.044	109.83	0.26
		0.2	0.217	108.32	1.40
		0.4	0.402	100.58	0.81
Strawberry	0	0.02	0.021	104.55	0.13
		0.04	0.041	101.86	0.19
		0.2	0.195	97.28	3.68
		0.4	0.376	94.07	1.33
Kiwi (unripe)	0	0.02	0.021	106.4	0.06
		0.04	0.041	103.39	0.08
		0.2	0.203	101.65	0.69
		0.4	0.403	100.63	1.89
Kiwi (ripe)	0.0938 ± 0.0027	—	—	—	—

recoveries ranged between 94.07–110.29% (Table 1). These results indicate that Probe **1** could accurately and quickly determine the β-gal activity in fruit.

4. Conclusions

In this study, a coumarin fluorescent probe (Probe **1**) was developed for the ratiometric detection of β-gal activity. The mechanism of β-gal recognition by Probe **1** involves the β-gal enzymatic hydrolysis of β-galactosides. The quantitative range of β-gal activity detected was 0–0.1 U mL^{-1} and 0.2–0.8 U mL^{-1}, with an LOD of 0.0054 U mL^{-1}. This method exhibited good linearity and specificity, had a short analytical time (30 min), required a small amount of sample (20 μL), and had a low LOD. Additionally, the luminous intensity of Probe **1** gradually increased with increasing enzyme activity. This phenomenon could be observed by the naked eye under 254 nm UV irradiation. Furthermore, Probe **1** was a useful tool for the qualitative and quantitative determination of β-gal activity in fruit.

Conflicts of interest

There are no conflicts of interest to declare.

Acknowledgements

Thank you for the National Natural Science Foundation of China (31901770).

References

1 Q. Husain, β Galactosidases and their potential applications: a review, *Crit. Rev. Biotechnol.*, 2010, **30**, 41–62.
2 Y. Tanaka, J. Kato, M. Kohara and M. S. Galinski, Antiviral effects of glycosylation and glucose trimming inhibitors on human parainfluenza virus type 3, *Antiviral Res.*, 2006, **72**, 1–9.
3 D. C. Vieira, L. N. Lima, A. A. Mendes, W. S. Adriano, R. C. Giordano, R. L. Giordano and P. W. Tardioli, Hydrolysis of lactose in whole milk catalyzed by β-galactosidase from Kluyveromyces fragilis immobilized on chitosan-based matrix, *Biochem. Eng. J.*, 2013, **81**, 54–64.
4 S. Rastegar, M. Rahemi, A. Baghizadeh and M. Gholami, Enzyme activity and biochemical changes of three date palm cultivars with different softening pattern during ripening, *Food Chem.*, 2012, **134**, 1279–1286.
5 F. Tidona, A. Meucci, M. Povolo, V. Pelizzola, M. Zago, G. Contarini, D. Carminati and G. Giraffa, Applicability of Lactococcus hircilactis and Lactococcus laudensis as dairy cultures, *Int. J. Food Microbiol.*, 2018, **271**, 1–7.
6 S. Mohebbi, M. Babalar, Z. Zamani and M. A. Askari, Influence of early season boron spraying and postharvest calcium dip treatment on cell-wall degrading enzymes and fruit firmness in 'Starking Delicious' apple during storage, *Sci. Hortic.*, 2020, **259**, 108822;
7 M. Ishimaru, D. L. Smith, A. J. Mort and K. C. Gross, Enzymatic activity and substrate specificity of recombinant tomato β-galactosidases 4 and 5, *Planta*, 2009, **229**, 447–456.
8 H. Lazan, S. Y. Ng, L. Y. Goh and Z. M. Ali, Papaya β-galactosidase/galactanase isoforms in differential cell wall hydrolysis and fruit softening during ripening, *Plant Physiol. Biochem.*, 2004, **42**, 847–853.
9 A. Weber, D. A. Neuwald, D. Kittemann, F. R. Thewes, V. Both and A. Brackmann, Influence of respiratory quotient dynamic controlled atmosphere (DCA–RQ) and ethanol

application on softening of Braeburn apples, *Food Chem.*, 2020, **303**, 125346.

10 A. Nakatsuka, T. Maruo, C. Ishibashi, Y. Ueda, N. Kobayashi, M. Yamagishi and H. Hiroyuki Itamura, Expression of genes encoding xyloglucan endotransglycosylase/hydrolase in 'Saijo' persimmon fruit during softening after deastringency treatment, *Postharvest Biol. Technol.*, 2011, **62**, 89–92;

11 A. B. Bennett and J. M. Labavitch, Ethylene and ripening-regulated expression and function of fruit cell wall modifying proteins, *Plant Sci.*, 2008, **175**, 130–136.

12 B. G. Defilippi, T. Ejsmentewicz, M. P. Covarrubias, O. Gudenschwager and R. Campos-Vargas, Changes in cell wall pectins and their relation to postharvest mesocarp softening of "Hass" avocados (Persea americana Mill.), *Plant Physiol. Biochem.*, 2018, **128**, 142–151.

13 A. Tateishi, H. Inoue, H. Shiba and S. Yamaki, Molecular cloning of β-galactosidase from Japanese pear (Pyrus pyrifolia) and its gene expression with fruit ripening, *Plant Cell Physiol.*, 2001, **42**, 492–498.

14 S. Guo, J. Song, B. Zhang, H. Jiang, R. Ma and M. Yu, Genome-wide identification and expression analysis of beta-galactosidase family members during fruit softening of peach [*Prunus persica* (L.) Batsch], *Postharvest Biol. Technol.*, 2018, **136**, 111–123.

15 X. Zheng, G. Jing, Y. Liu, T. Jiang, Y. Jiang and J. Li, Expression of expansin gene, MiExpA1, and activity of galactosidase and polygalacturonase in mango fruit as affected by oxalic acid during storage at room temperature, *Food Chem.*, 2012, **132**, 849–854.

16 S. Boelz, G. Neu-Yilik, N. H. Gehring, M. W. Hentze and A. E. Kulozik, A chemiluminescence-based reporter system to monitor nonsense-mediated mRNA decay, *Biochem. Biophys. Res. Commun.*, 2006, **349**, 186–191.

17 D. Farquhar, B. Pan, M. Sakurai, A. Ghosh, C. A. Mullen and A. J. Nelson, Suicide gene therapy using E. coli β-galactosidase, *Canc. Chemother. Pharmacol.*, 2002, **50**, 65–70.

18 J. Chen, Z. Jiang, J. D. Ackerman, M. Yazdani, S. Hou, S. R. Nugen and V. M. Rotello, Electrochemical nanoparticle–enzyme sensors for screening bacterial contamination in drinking water, *Analyst*, 2015, **140**, 4991–4996.

19 A. Y. Louie, M. M. Hüber, E. T. Ahrens, U. Rothbächer, R. Moats, R. E. Jacobs, S. E. Fraser and T. J. Meade, In vivo visualization of gene expression using magnetic resonance imaging, *Nat. Biotechnol.*, 2000, **18**, 321–325.

20 G. Andreotti, A. Trincone and A. Giordano, Convenient synthesis of β-galactosyl nucleosides using the marine β-galactosidase from Aplysia fasciata, *J. Mol. Catal. B: Enzym.*, 2007, **47**, 28–32.

21 S. J. Kim, D. J. Doudet, A. R. Studenov, C. Nian, T. J. Ruth, S. S. Gambhir and C. H. S. McIntosh, Quantitative micro positron emission tomography (PET) imaging for the *in vivo* determination of pancreatic islet graft survival, *Nat. Med.*, 2006, **12**, 1423–1428.

22 T. Naqvi, A. Lim, R. Rouhani, R. Singh and R. M. Eglen, Galactosidase enzyme fragment complementation as a high-throughput screening protease technology, *J. Biomol. Screen*, 2004, **9**, 398–408.

23 T. Tschirhart, X. Y. Zhou, H. Ueda, C. Y. Tsao, E. Kim, G. F. Payne and W. E. Bentley, Electrochemical measurement of the β-galactosidase reporter from live cells: a comparison to the Miller assay, *ACS Synth. Biol.*, 2016, **5**, 28–35.

24 X. Kong, M. Li, B. Dong, Y. Yin, W. Song and W. Lin, An ultrasensitivity fluorescent probe based on the ICT-FRET dual mechanisms for imaging β-galactosidase *in vitro* and *ex vivo*, *Anal. Chem.*, 2019, **91**, 15591–15598.

25 J. Liu, H. Bao, C. Liu, F. Wu and F. Gao, "Turn-On" Fluorescence Determination of β-Glucosidase Activity Using Fluorescent Polymer Nanoparticles Formed from Polyethylenimine Cross-Linked with Hydroquinone, *ACS Appl. Polym. Mater.*, 2019, **1**, 3057–3063.

26 J. Zhang, P. Cheng and K. Pu, Recent Advances of Molecular Optical Probes in Imaging of β-Galactosidase, *Bioconjugate Chem.*, 2019, **30**, 2089–2101.

27 R. Gui, H. Jin, X. Bu, Y. Fu, Z. Wang and Q. Liu, Recent advances in dual-emission ratiometric fluorescence probes for chemo/biosensing and bioimaging of biomarkers, *Coord. Chem. Rev.*, 2019, **383**, 82–103.

28 X. Bu, Y. Fu, X. Jiang, H. Jin and R. Gui, Self-assembly of dna-templated copper nanoclusters and carbon dots for ratiometric fluorometric and visual determination of arginine and acetaminophen with a logic-gate operation, *Microchim. Acta*, 2020, **187**, 154.

29 X. Jiang, H. Jin, Y. Sun, Z. Sun and R. Gui, Assembly of black phosphorus quantum dots-doped mof and silver nanoclusters as a versatile enzyme-catalyzed biosensor for solution, flexible substrate and latent fingerprint visual detection of baicalin, *Biosens. Bioelectron.*, 2020, **152**, 112012.

30 H. W. Liu, L. Chen, C. Xu, Z. Li, H. Zhang, X. B. Zhang and W. Tan, Recent progresses in small-molecule enzymatic fluorescent probes for cancer imaging, *Chem. Soc. Rev.*, 2018, **47**, 7140–7180.

31 N. Hananya, A. Eldar Boock, C. R. Bauer, R. Satchi-Fainaro and D. Shabat, Remarkable Enhancement of Chemiluminescent Signal by Dioxetane−Fluorophore Conjugates: Turn-ON Chemiluminescence Probes with Color Modulation for Sensing and Imaging, *J. Am. Chem. Soc.*, 2016, **138**, 13438–13446.

32 T. S. Wehrman, G. von Degenfeld, P. O. Krutzik, G. P. Nolan and H. M. Blau, Luminescent Imaging of β-Galactosidase Activity in Living Subjects using Sequential Reporter-Enzyme Luminescence. Nat, *Methods*, 2006, **3**, 295–301.

33 H. W. Lee, C. H. Heo, D. Sen, H. O. Byun, I. H. Kwak, G. Yoon and H. M. Kim, Ratiometric Two-Photon Fluorescent Probe for Quantitative Detection of β-Galactosidase Activity in Senescent Cells, *Anal. Chem.*, 2014, **86**, 10001–10005.

34 B. Lozano-Torres, I. Galiana, M. Rovira, E. Garrido, S. Chaib, A. Bernardos, D. Muñoz-Espín, M. Serrano, R. Martínez-Máñez and F. Sancenón, An OFF–ON Two-Photon Fluorescent Probe for Tracking Cell Senescence in Vivo, *J. Am. Chem. Soc.*, 2017, **139**, 8808–8811.

35 K. Gu, Y. Xu, H. Li, Z. Guo, S. Zhu, S. Zhu, P. Shi, T. D. James, H. Tian and W. H. Zhu, Real-Time Tracking and *In Vivo* Visualization of β-Galactosidase Activity in Colorectal Tumor with a Ratiometric Near-Infrared Fluorescent Probe, *J. Am. Chem. Soc.*, 2016, **138**, 5334–5340.

36 E. J. Kim, R. Kumar, A. Sharma, B. Yoon, H. M. Kim, H. Lee, K. S. Hong and J. S. Kim, In Vivo Imaging of β-Galactosidase Stimulated Activity in Hepatocellular Carcinoma using Ligand-Targeted Fluorescent Probe, *Biomaterials*, 2017, **122**, 83–90.

37 C. H. Tung, Q. Zeng, K. Shah, D. E. Kim, D. Schellingerhout and R. Weissleder, In Vivo Imaging of β-Galactosidase Activity Using Far Red Fluorescent Switch, *Cancer Res.*, 2004, **64**, 1579–1583.

38 D. Oushiki, H. Kojima, Y. Takahashi, T. Komatsu, T. Terai, K. Hanaoka, M. Nishikawa, Y. Takakura and T. Nagano, Near-Infrared Fluorescence Probes for Enzymes Based on Binding Affinity Modulation of Squarylium Dye Scaffold, *Anal. Chem.*, 2012, **84**, 4404–4410.

39 J. Zhang, C. Li, C. Dutta, M. Fang, S. Zhang, A. Tiwari, F. Luo and H. Liu, A novel near-infrared fluorescent probe for sensitive detection of β-galactosidase in living cells, *Anal. Chim. Acta*, 2017, **968**, 97–104.

40 Y. Li, N. Duan, X. Wu, S. Yang, H. Tian and B. Sun, Novel fluorescent probe for the ratiometric detection of β-galactosidase and its application in fruit, *Food Chem.*, 2020, **328**, 127112.

41 N. Duan, H. Wang, Y. Li, S. Yang, H. Tian and B. Sun, The research progress of organic fluorescent probe applied in food and drinking water detection, *Coord. Chem. Rev.*, 2021, **427**, 213557.